TISSUE ENGINEERING: Part A
Volume 17, Numbers 7 and 8, 2011
© Mary Ann Liebert, Inc.
DOI: 10.1089/ten.tea.2010.0294

# A Bilayer Construct Controls Adipose-Derived Stem Cell Differentiation into Endothelial Cells and Pericytes Without Growth Factor Stimulation

Shanmugasundaram Natesan, Ph.D.,[1] Ge Zhang, M.D., Ph.D.,[2] David G. Baer, Ph.D.,[1] Thomas J. Walters, Ph.D.,[1] Robert J. Christy, Ph.D.,[1] and Laura J. Suggs, Ph.D.[3]

This work describes the differentiation of adipose-derived mesenchymal stem cells (ASC) in a composite hydrogel for use as a vascularized dermal matrix. Our intent is that such a construct could be utilized following large-surface-area burn wounds that require extensive skin grafting and that are limited by the availability of uninjured sites. To develop engineered skin replacement constructs, we are pursuing the use of ASC. We have established that a PEGylated fibrin gel can provide a suitable environment for the proliferation of ASC over a 7 day time course. Further, we have demonstrated that PEGylated fibrin can be used to control ASC differentiation toward vascular cell types, including cells characteristic of both endothelial cells and pericytes. Gene expression analysis revealed strong upregulation of endothelial markers, CD31, and von Willebrand factor, up to day 11 in culture with corresponding evidence of protein expression demonstrated by immunocytochemical staining. ASC were not only shown to express endothelial cell phenotype, but a subset of the ASC expressed pericyte markers. The NG2 gene was upregulated over 11 days with corresponding evidence for the cell surface marker. Platelet-derived growth factor receptor beta gene expression decreased as the multipotent ASC differentiated up to day 7. Increased receptor expression at day 11 was likely due to the enhanced pericyte gene expression profile, including increased NG2 expression. We have also demonstrated that when cells are loaded onto chitosan microspheres and sandwiched between the PEGylated fibrin gel and a type I collagen gel, the cells can migrate and proliferate within the two different gel types. The matrix composition dictates the lineage specification and is not driven by soluble factors. Utilizing an insoluble bilayer matrix to direct ASC differentiation will allow for the development of both vasculature as well as dermal connective tissue from a single population of ASC. This work underscores the importance of the extracellular matrix in controlling stem cell phenotype. It is our goal to develop layered composites as wound dressings or vascularized dermal equivalents that are not limited by nutrient diffusion.

## Introduction

Recent advances in tissue engineering-based wound dressings[1] have resulted in the emergence of a range of dermal, epidermal, and even complete skin equivalents.[2] These products have proven useful in a wide variety of wound care applications; however, significant challenges remain, especially for larger wounds such as extensive burns.[3] Of particular interest is the growth of a robust blood vessel network to perfuse living cells within skin equivalents. This challenge, in combination with the time required to grow significant numbers of autologous cells, has limited the clinical utility of the current products. The present strategy would allow for the formation of both blood vessels and dermal connective tissue from a uniform cell population that could be seeded and spontaneously assemble without the need for long culture times, high costs, and problematic *ex vivo* culture.

Currently, research on stem cells, such as epidermal stem cells, dermal stem cells, and mesenchymal stem cells (MSC) from bone marrow, may provide technologies for the functional repair and regeneration of skin.[4] A multipotent MSC population has been described from the stromal fraction of adipose tissue and may be useful in the repair and reconstruction of multiple tissue types.[5,6] MSC derived from adipose tissues (ASC) differentiate into multiple phenotypes, including adipose, muscle, bone, neuronal, endothelial, hepatocyte, and epithelial-like cells.[7–11] Adipose-derived stem

[1]Regenerative Medicine Research Program, U.S. Army Institute of Surgical Research, Fort Sam Houston, Texas.
[2]Department of Biomedical Engineering, Olson Research Center, University of Akron, Akron, Ohio.
[3]Department of Biomedical Engineering, The University of Texas at Austin, Austin, Texas.

# Report Documentation Page

*Form Approved*
*OMB No. 0704-0188*

Public reporting burden for the collection of information is estimated to average 1 hour per response, including the time for reviewing instructions, searching existing data sources, gathering and maintaining the data needed, and completing and reviewing the collection of information. Send comments regarding this burden estimate or any other aspect of this collection of information, including suggestions for reducing this burden, to Washington Headquarters Services, Directorate for Information Operations and Reports, 1215 Jefferson Davis Highway, Suite 1204, Arlington VA 22202-4302. Respondents should be aware that notwithstanding any other provision of law, no person shall be subject to a penalty for failing to comply with a collection of information if it does not display a currently valid OMB control number.

| 1. REPORT DATE | 2. REPORT TYPE | 3. DATES COVERED |
|---|---|---|
| **01 APR 2011** | **N/A** | **-** |

| 4. TITLE AND SUBTITLE | 5a. CONTRACT NUMBER |
|---|---|
| **A bilayer construct controls adipose-derived stem cell differentiation into endothelial cells and pericytes without growth factor stimulation** | 5b. GRANT NUMBER |
| | 5c. PROGRAM ELEMENT NUMBER |
| 6. AUTHOR(S) | 5d. PROJECT NUMBER |
| **Natesan S., Zhang G., Baer D. G., Walters T. J., Christy R. J., Suggs L. J.,** | 5e. TASK NUMBER |
| | 5f. WORK UNIT NUMBER |
| 7. PERFORMING ORGANIZATION NAME(S) AND ADDRESS(ES) | 8. PERFORMING ORGANIZATION REPORT NUMBER |
| **United States Army Institute of Surgical Research, JBSA Fort Sam Houston, TX** | |
| 9. SPONSORING/MONITORING AGENCY NAME(S) AND ADDRESS(ES) | 10. SPONSOR/MONITOR'S ACRONYM(S) |
| | 11. SPONSOR/MONITOR'S REPORT NUMBER(S) |

12. DISTRIBUTION/AVAILABILITY STATEMENT
**Approved for public release, distribution unlimited**

13. SUPPLEMENTARY NOTES

14. ABSTRACT

15. SUBJECT TERMS

| 16. SECURITY CLASSIFICATION OF: | | | 17. LIMITATION OF ABSTRACT | 18. NUMBER OF PAGES | 19a. NAME OF RESPONSIBLE PERSON |
|---|---|---|---|---|---|
| a. REPORT | b. ABSTRACT | c. THIS PAGE | | | |
| **unclassified** | **unclassified** | **unclassified** | **UU** | **14** | |

cells are easily isolated from the stromal vasculature of subcutaneous adipose tissue by liposuction with a minimally invasive procedure. Relative to the stem cell population within bone marrow, it has been reported that adipose tissue contains 100–1000 times more cells.[12] This makes adipose tissue an attractive *in vivo* cellular source of autologous stem cells for regenerative therapies especially for those where an *in vitro* expansion step is problematic. Recently, ASC have been used to modulate the skin wound healing process, especially the aspect of fibroblast activation proliferation, collagen synthesis, and migratory properties. Moreover, ASC showed a stimulatory effect on migration of human dermal fibroblasts in *in vitro* wound healing models.[13] The wound healing effects of ASC were also verified with an *in vivo* animal study, demonstrating that ASC significantly reduced wound size and accelerated re-epithelialization.[13]

Still, a major challenge remaining in the regeneration and repair of large soft-tissue trauma is delivery of cells to the wound site in a three-dimensional (3D) biocompatible and biodegradable matrix in which cells can proliferate and differentiate. Fibrin is a versatile biopolymer formed after thrombin-mediated cleavage of fibrinopeptide A from monomeric fibrinogen.[14] Fibrin and fibrinogen have critical roles in blood clotting, fibrinolysis, cellular and matrix interactions, the inflammatory response, wound healing, and neoplasia.[15] Fibrin has been used clinically as an U.S. Food and Drug Administration–approved hemostatic agent and as a sealant in a variety of clinical applications, including procedures such as soft tissue dissection. Fibrin hydrogels from commercially purified allogeneic fibrinogen and thrombin have been used widely in the last decade in a variety of tissue engineering applications, and these include tissue engineering of adipose[16] cardiovascular[15,17–20] ocular,[21–23] muscle,[24–27] and skin.[28,29] In addition, fibrin hydrogels have applications for promoting angiogenesis.[30–32] Major disadvantages with fibrin as a potential scaffold are low mechanical stiffness and its rapid degradation before the proper formation of tissue-engineered structures.[15] To overcome these problems, fibrin can be modified before use to serve as a better 3D tissue engineering scaffold. One such approach is the copolymerization of fibrin with polyethlylene glycol.[33–36] Our prior work has demonstrated several unique features of PEGylated fibrin that make it advantageous in wound healing over other hydrogel dressings.

Clinical trials aimed at delivering growth factors in an effort to enhance new blood vessel growth to enhance wound healing have been disappointing.[37–39] It has been observed that this failure is due, in part, to the transient nature of the angiogenic response. While delivered growth factors could indeed stimulate significant early blood vessel ingrowth, the resulting structures did not receive the necessary stabilization cues to prevent vascular regression. Formation of mature vascular beds by normal developmental processes is a complex sequence of events requiring precise regulation of progenitor cell mobilization and differentiation both spatially and temporally. It is therefore a target of this project to modulate rapid, mature vascularization to improve the outcomes of wound healing. In the present study, we evaluated the ability of PEGylated fibrin to control the vascular differentiation of ASC. We have combined this hydrogel with a collagen gel in a bilayer construct in an effort to approximate both the dermal connective tissue as well as the vascular bed to nourish it (Fig. 1). We have employed a previously described system based on the use of chitosan microbeads as a cell carrier to place the ASC within the bilayer gel construct. The matrix-dependent control of ASC differentiation was then evaluated.

## Materials and Methods

### *Isolation of adipose-derived stem cells*

Rat ASC were isolated from perirenal and epididymal adipose tissue as previously described.[11,40] Perirenal and epididymal adipose tissue was collected and washed with sterile Hanks buffered balance solution (HBBS) containing 1% bovine serum albumin. The tissue was minced, transferred into 25 mL of HBBS, and centrifuged (500 *g* at room temperature for 10 min). The free floating adipose tissue layer was collected, and transferred to 25 mL of HBSS containing 1% fetal bovine serum and 200 U/mL of collagenase type II (Sigma-Aldrich, St. Louis, MO) for 45 min at 37°C in an orbital shaker. The digested tissue was then filtered through 100 and 70 μm nylon mesh filter, centrifuged for 10 min at 500 *g* at room temperature, and washed twice with sterile HBBS. The cell pellet was re-suspended in growth media (MesenPRO RS™ Basal Medium, supplemented with MesenPRO RS Growth Supplement, antibiotic–antimycotic [100 U/mL of penicillin G, 100 μg/mL streptomycin sulfate, and 0.25 μg/mL Amphotericin B], and 2 mM L-glutamine [GIBCO, Invitrogen, Carlsbad, CA]). Cells were cultured on T75 flasks (BD Falcon, Franklin Lakes, NJ) and maintained in a 5% $CO_2$ humidified incubator at 37°C. Passage 2–4 ASC were used for all experiments.

### *Immunocytochemistry of stem cell surface markers*

ASC were incubated on a two-well-chambered slide (Nalge Nunc, LabTek® chamber slide, Noperville, IL) for 48 h. The cells were washed twice with sterile HBSS and fixed with 4% paraformaldehyde (PFA) for 15 min. Fc receptor-mediated blocking sites were blocked by incubating the cells for 20 min with (1 μg/$10^4$ cells) of BD Fc Block™ Solution (BD Bioscience, San Jose, CA) or nonpermeant

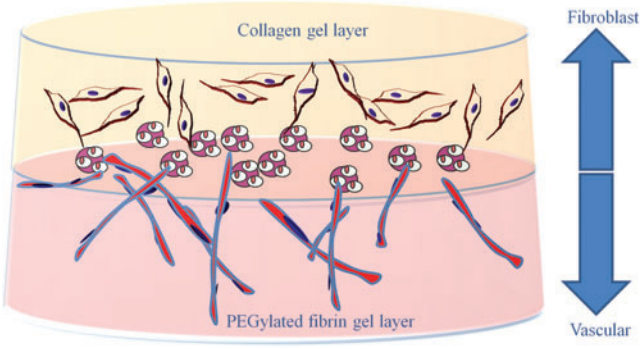


**FIG. 1.** Schematic of a layered construct that could provide both the vascular as well as dermal fibroblast component for treatment of wounds. The bilayer construct would consist of two different hydrogel matrices controlling adipose-derived mesenchymal stem cell (ASC) differentiation. ASC could be seeded on microcarriers and either migrate into the matrix or the carriers could be seeded within the matrix. Color images available online at www.liebertonline.com/tea.

blocking solution containing 5% donkey serum (Sigma, St. Louis, MO) in HBSS. Stem cell surface markers were identified by incubating ASC overnight, 4°C, with 10 μg of fluorescein isothiocyanate (FITC)-conjugated anti-mouse monoclonal antibodies against CD54 (ICAM-1), CD71 (transferrin receptor), CD 49d (integrin α4), and CD90 (Thy-1 glycoprotein) (BD Bioscience). To observe STRO-1 (R&D Systems, Minneapolis, MN) expression, cells were fixed with 4% PFA for 15 min, washed twice with phosphate-buffered saline (PBS), blocked with 2% serum, and incubated overnight at 4°C with 10 μg of STRO-1. The cells were washed twice with PBS and incubated 45 min at 4°C with 5 μg/mL of FITC-labeled anti-mouse IgM secondary reagent (R&D Systems). Nonspecific fluorescence was determined using ASC incubated with FITC-labeled Ig class secondary antibody reagents.

### *Preparation of ASC-seeded PEGylated fibrin gel*

PEGylated fibrinogen was prepared as per our previous procedure[36] with slight modification. Succinimidyl glutarate-modified polyethylene glycol (SG-PEG-SG, 3400 Da; NOF America Corporation, White Plains, NY) was added to fibrinogen (Sigma-Aldrich) in a molar concentration ratio of 1:10, SG-PEG-SG: fibrinogen, in tris-buffered saline, pH 7.8, and incubated for 20 min at 37°C. An equal volume of thrombin (Sigma-Aldrich) in 40 mM $CaCl_2$ at a final concentration of 10 U/mL was added and incubated for 10 min at 37°C. The resulting gels were then rinsed with tris-buffered saline (pH 7.8) to remove unbound free SG-PEG-SG. To prepare ASC-seeded gels, cells of at different concentrations (5000–50,000/gel) were added to PEG-fibrinogen mixture before the initiation of gelation with thrombin. The cell–gel mixture was placed in a 12-well plate and incubated at 37°C for 10 min. After complete gelation, the PEGylated fibrin gels were washed twice with HBSS and incubated with alpha minimal essential media supplemented with 10% fetal bovine serum, antibiotic–antimycotic (100 U/mL of penicillin G, 100 (g/mL streptomycin sulfate, and 0.25 (g/mL amphotericin B), and 2 mM L-glutamine (Invitrogen, Carlsbad, CA), in a 5% $CO_2$ humidified incubator at 37°C.

### *Morphological analysis and viability of ASC in PEGylated fibrin gel*

ASC seeded at different concentrations (5000–50,000 cells) in PEGylated fibrin gel were observed, and photomicrographs were taken at different time points (1, 3, 5, and 7 days) using an Olympus IX71 inverted microscope equipped with reflected fluorescence system and DP71 digital camera (Olympus America Inc., Center Valley, PA). At similar time points the growth medium was removed and 50 μL MTT (3-(4,5-dimethylthiozole-2-yl)-2,5-diphenyltetrazolium bromide; Sigma-Aldrich) solution (5 mg/mL) was added to each gel and incubated for 5 h in a 5% $CO_2$ humidified incubator at 37°C.[41] After incubation the MTT solution was removed and 500 μL of isopropyl-acetone mixture (1:1) was added and allowed to incubate for 30 min to solubilize and extract the formazan complex. The gel–solvent mixture was then centrifuged at 2700 *g* for 10 min and the supernatant was collected and added to individual wells of a 24-well plate. Absorbance of the supernatants and isopropyl alcohol–acetone mixture (reagent blank) was measured at 570 with 630 nm as reference using Molecular Devices Spectramax M2 Microplate Reader (Molecular Devices, Sunnyvale, CA). The cell number associated with PEGylated fibrin gel was determined relative to the standard absorbance value obtained from known numbers of viable ASC.

### *Immunocytochemical analysis of ASC-seeded PEGylated fibrin gels*

**Immunostaining of ASC in PEGylated fibrin gels.** Before cryosectioning, gels (day 11) were cryopreserved using gradient sucrose cryopreservation technique.[42] Briefly, the gels were washed with HBSS (twice, 5 min), fixed with 4% PFA (EMS, Hatfield, PA), treated serially with increasing concentrations of sucrose (from 5% to 20%), and then incubated overnight with 20% sucrose at 4°C. The sucrose-treated gels were embedded in a 20% Sucrose-Histoprep™ (Fisher, Pittsburgh, PA) mixture (2:1) and flash frozen. Sections, 10–12 μm thick, were cut using a cryostat (Leica Microsystems, Nussloch, Germany), washed with sterile HBSS, and fixed with 4% PFA for 20 min. Nonspecific Fc receptor-mediated blocking sites were blocked by incubating the sections for 40 min—1 h with 1% bovine serum albumin in HBSS containing 0.01% Triton×100 and washed twice (5 min) with HBSS. To assess the endogenic immunophenotype, sections were stained with anti rat CD31 (PECAM-1, 8 μg/mL; R&D Systems) and von Willebrand factor (vWF, 10 μg/mL; Millipore, Billerica, MA)–specific monoclonal primary antibodies. For identifying pericyte immunophenotype, rat-specific monoclonal antibodies specific to chrondroitin sulfate proteoglycan (NG2, 20 μg/mL; Millipore), platelet-derived growth factor receptor beta (PDGFRβ, 10 μg/mL; R&D Systems), and alpha smooth muscle actin (α-SMA, 8 μg/mL; Abcam, Cambridge, MA) antibodies were used. The sections were subjected to single or double immunofluorescent staining by incubating with a monoclonal primary antibody or mixture of two antibodies targeted toward two different antigens at 4°C overnight. After incubation of unconjugated primary labeled antibodies, sections were washed twice (5 min) with HBSS and incubated with 5 μg/mL host species-specific Alexa fluor 488 and/or Alexa fluor 594 secondary antibodies (Invitrogen) for 45 min at 4°C. Finally, the sections were washed twice (5 min) and nuclei stained with Hoechst 33342 (Invitrogen). Nonspecific fluorescence was determined using sections incubated with respective fluorophore-labeled secondary antibodies.

**Fluorescent and confocal microscopic morphological analysis.** Epifluorescence of cells and gel sections were observed using Olympus IX71 inverted microscope equipped with reflected fluorescence system (Olympus America Inc.). Photomicrographs were taken using DP71 digital camera and image overlay was carried out using DP controller application software. Three-dimensional images were taken using an Olympus FV-500 Laser Scanning Confocal Microscope (Olympus America Inc.), equipped with a three-channel detection system for fluorescence, a differential interference contrast image laser light source, and a Z-stepper motor. The 3D stereoscopic images and movie were generated from a series of Z-stacked photomicrographs around the Z-axis using Fluoview and Tiempo Ratio Imaging software and final images processed using ImageJ software (image processing and analysis in Java; NIH, Bethesda, MD).

### *Transmission electron microscopy*

ASC cultured in PEGylated fibrin gel (11 days postculture) were fixed in 1% v/v glutaraldehyde in PBS. The samples were rinsed in 0.1 M, pH 7.4 phosphate buffer (two times, 3 min each) and then placed in 1% Zetterquist's Osmium for 30 min. The samples were subsequently dehydrated in a series of ethanol washes (70% for 10 min, 95% for 10 min, and 100% for 20 min), treated with hexamethyldisilizane (two times, 5 min each), and finally air-dried in a desiccator. Samples were then washed and infiltrated with epoxy resin. Ultrathin sections (~70 nm) were cut and sections were examined on a JOEL 1230 transmission electron microscope.

### *RNA isolation and real-time polymerase chain reaction*

Total RNA from ASC in PEGylated fibrin gel at 1, 3, 5, 7, and 11 days were isolated using Trizol LS reagent (Invitrogen) with modifications.[43] Gels were rinsed with HBSS and carefully removed from the culture well. Four gels from each time were pooled together and minced, and 16 mL of Trizol LS reagent was added and incubated for 10–15 min in ice. After incubation 8 mL of chloroform was added and mixed, and the aqueous phase separated by centrifugation. The RNA was then purified using mini spin columns. The concentration and quality of the purified RNA was determined at $OD_{260/280}$ using a NanoDrop spectrometer (Nanodrop Technologies, Inc., Wilmington, DE). Complementary DNA was synthesized from 150 ng of total RNA, in duplicate, using SuperScript™ III first strand synthesis supermix with oligo-dT primers (Invitrogen). A control lacking the RNA sample was synthesized to detect the random production of cDNA through contaminants. Oligonucleotide primer sequences specific to endothelial (CD31 and vWF) and pericyte markers (NG2 and PDGFRβ) were purchased from SA Biosciences (Frederick, MD). Master mixes containing 200 nM of forward and reverse primers with SYBR® GreenER™, qPCR supermix (Invitrogen), and the synthesized cDNA were added to appropriate wells. Real-time polymerase chain reaction (RT-PCR) was carried out using a Bio-Rad CFX96 thermal cycler system (Bio-Rad, Hercules, CA). mRNA expression levels were normalized to glyceraldehye-3-phosphate dehydrogenase. Fold increase in expression levels for each endogenic and pericyte specific gene was normalized to the expression levels of control passage 2 ASC.[44] Fold increase in expression levels for each gene was determined by $2^{-\Delta\Delta C}{}_{T}$ method.[44]

### *Impregnation of ASC-loaded chitosan microspheres in PEGylated fibrin and collagen gels*

Loading ASC into chitosan microspheres. Chitosan microspheres (CSM) were prepared by water in oil emulsification process along with an ionic coacervation technique using our previous described protocol.[45] Prepared CSM were sterilized using absolute alcohol and washed (three times) with sterile water to remove residual salts. ASC were loaded into CSM at 10,000 cells/mg using our culture insert technique as previously described.[45] Before culturing ASC in CSM, the cells were cytoplasmically labeled with Quantum dot (Qdot) nanocrystals 565 using Qtracker cell labeling kit (Invitrogen). Cells were labeled according to manufacturer's instructions: briefly, 2 μL of labeling solution containing 10 nM of Qdots was incubated for 5 min at 37°C and to this solution 200 μL of MesenPRO medium was added and vortexed. To this solution mixture, 1 mL of cell suspension ($1\times10^6$ cells/mL) was added and incubated for 45 min at 37°C, 5% $CO_2$. After incubation, labeled cell suspension was diluted with MesenPRO media to a final concentration of $5\times10^4$ cells/200 μL and seeded over sterilized CSM (5 mg), spread over culture insert of 8 μm pore size membrane (24-well format; BD Falcon), and incubated for 24 h in a humidified incubator at 37°C and 5% $CO_2$.

Impregnation procedure. ASC (with and without Qdot label)-loaded CSM (5 mg) were collected and mixed with PEGylated fibrin gel matrix (prepared as described earlier). The PEGylated fibrin-ASC-CSM mixture was added to a 12-well plate and incubated for 10 min at 37°C. In another experimental setup, ASC (with and without Qdot label)-loaded CSM (5 mg) were collected and impregnated into collagen type I gels following our previous procedure.[45] Briefly, type 1 collagen (5 mg/mL; Travigen, Gaithersburg, MD) from rat tail tendon was fibrillated by adjusting the pH to 6.8–7.0 using 100 μL of Dulbecco's PBS and 23 μL of 1 N NaOH. The fibrillated collagen-ASC-CSM mixture was added to a 12-well plate and incubated for 30 min at 37°C. After complete gelation, both the gels (PEGylated fibrin and collagen gels) were incubated at 37°C, 5% $CO_2$. Release of cells was observed for 8 days in case of PEGylated fibrin gels, whereas in collagen gels cells were observed for 12 days and light microscopic pictures were taken at different days using Olympus IX71 inverted microscope equipped with reflected fluorescence system. To track cells and show their release into the gels, fluorescence micrographs were taken on day 6 in both the gels.

### *Development of bilayered PEGylated fibrin–(ASC-CSM)–collagen gel constructs*

To develop the bilayer construct, PEGylated fibrin gel was prepared as previously described and added to a six-well culture insert. Over the surface of the PEGylated fibrin gel 5 mg of ASC-loaded CSM (10,000 cells/mg) suspended in culture media (200 μL) was seeded onto the gel. After the microsphere has settled over the gel, fibrillated type 1 collagen, prepared as previously described, was carefully applied over the PEGylated fibrin–(ASC-CSM) platform before gelation, after which the whole construct was placed for 30 min at 37°C to achieve complete gelation of collagen matrix. The final bilayered construct consisted of PEGylated fibrin–(ASC-CSM)–collagen gel matrix, with collagen gel on the top surface, PEGylated fibrin gel on the bottom, and the ASC-loaded CSM sandwiched in the interface. The entire bilayered construct was incubated at 37°C, 5% $CO_2$ for 12 days, during which cells released into the gels were observed and photomicrographs were taken at different days to assess the morphology of the released cells into the gel matrix.

## Results

### *Undifferentiated ASC*

The phenotype of undifferentiated ASC has been described by our group and others with respect to cell surface marker expression measured with fluorescence activated cell sorting (FACS). These cells are positive for CD49d, CD54,

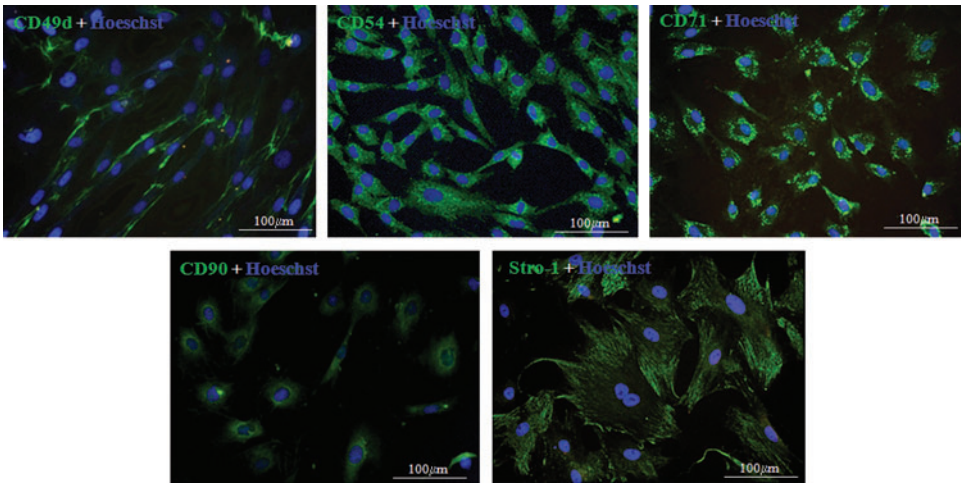


**FIG. 2.** Immunocytochemical analysis of ASC isolated from rats. Photomicrographs of markers expressed in third-passage ASC. Figures in each panel indicate the specific cell surface marker. All antibodies, except Stro-1, are fluorescein isothiocyanate-labeled primary antibodies. Stro-1 is identified using isotype-matched fluorescein isothiocyanate-labeled rat IgM. Color images available online at www.liebertonline.com/tea.

CD71, CD90, and STRO-1. Before the utilization of a particular cell population the positive expression of these five markers was confirmed using immunocytochemical staining. An example result for the cell populations used in this study is shown in Figure 2.

### *ASC growth characteristics within PEGylated fibrin*

Crosslinking of the PEGylated fibrin with embedded ASC results in no observable loss of cells into the media. ASC were observed throughout the gel as single cells. Much like bone-marrow-derived MSC, ASC demonstrate the ability to proliferate and express a characteristic phenotype within PEGylated fibrin gels. Figure 3 shows the dependency of cell seeding density and culture time on the resulting cell morphology. ASC began to exhibit cellular extensions by day 3. These extensions were more pronounced in cultures with >10,000 cells/mL. Over time the cellular extensions progressed with the formation of dense multicellular networks. By day 7, ASC at all seeding densities demonstrated

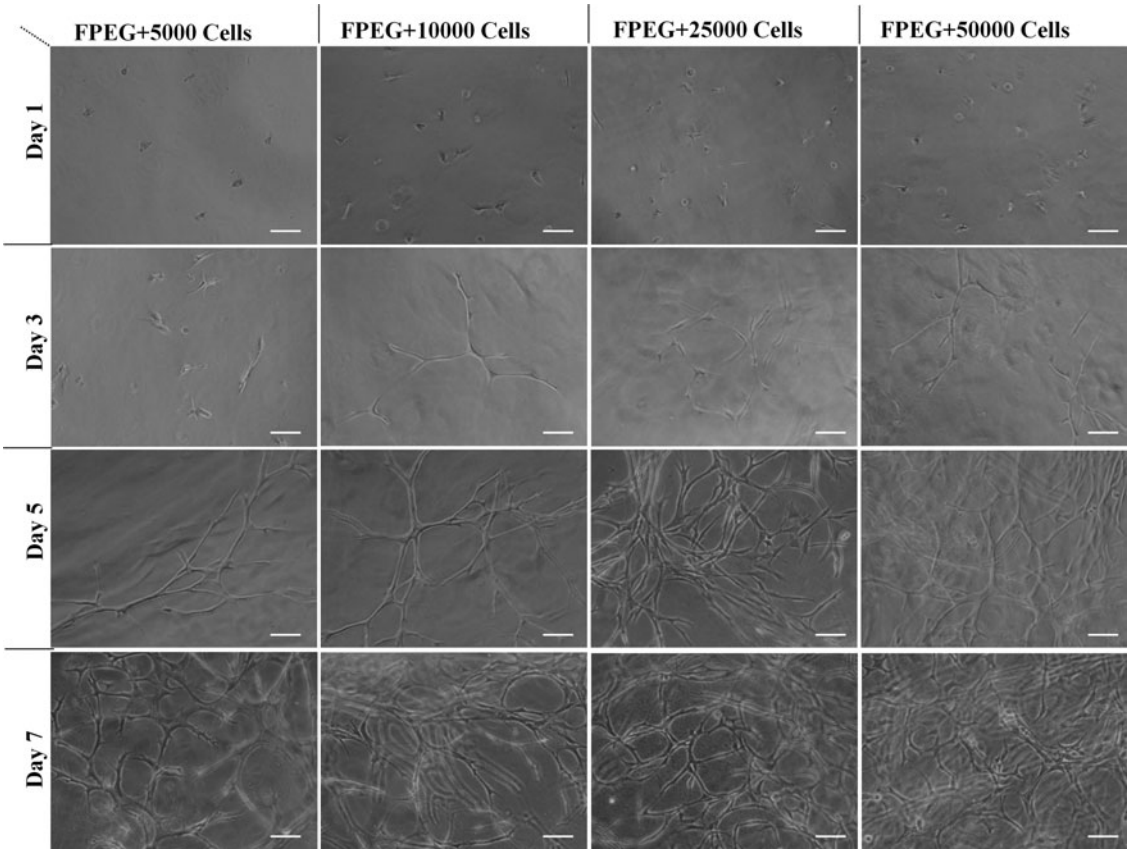


**FIG. 3.** Light microscopic images of differentiation time course of ASC into vascular like structures. Cells began to form vascular tube-like networks in the PEGylated fibrin gel in the absence of additional soluble cytokines. The amount of network formation was related to the initial cell density. Scale bar = 100 μm.

extensive network formation, which was greatest at the highest cell density. Proliferation was assessed over the same time course using the MTT assay (Fig. 4). Proliferative activity increased over the 7-day study for all seeding densities and was dependent on the initial density. A one-way analysis of variance demonstrated significant differences among different seeding densities at days 3 and 7 with $p < 0.005$.

### *ASC phenotype and genotype within PEGylated fibrin*

The endothelial cell markers, CD31 and vWF were used to establish the identity of cells expressing an endothelial cell genotype and phenotype. RT-PCR demonstrated that over the 11 day time course, there was a dramatic upregulation of endothelial cell markers relative to the housekeeping gene. Specifically, CD31 was upregulated 25-fold over controls, whereas vWF was up 42-fold over controls (Fig. 5). The immunohistochemical staining confirmed the presence of the expressed protein for both CD31 and vWF (Fig. 6A–D). Confocal images of stained sections confirm that both markers are expressed on multicellular networks generated from day 11 samples. What was demonstrated is that the CD31 is more closely associated with the cell nucleus than the vWF. This may be due to the fact that CD31 is expressed on endothelial cell membranes, where vWF may be secreted from the cell and maintained within the fibrin network.

The pericyte markers NG2, PDGFRβ, and α-SMA were used to track the differentiation of ASC toward a pericyte, or mural cell, phenotype. RT-PCR after 11 days in culture demonstrated that the markers, NG2 and PDGFRβ, were upregulated by sixfold and ninefold, respectively, relative to controls. Here, undifferentiated ASC also express a basal level of PDGFRβ, which was approximately fivefold greater than controls. This value declined as the culture progressed reaching a minimum at day 7 before an increase at day 11. Immunohistochemistry revealed that multicellular networks at day 11 exhibited expression of both NG2 (Fig. 6E–H) and α-SMA (Fig. 6I–L). Further, a 3D Z-stack animation was created from sections stained with vWF and α-SMA individually to observe the tube architecture formed in the fibrin gels (Supplementary Videos S1 and S2; Supplementary Data are available online at www.liebertonline.com/tea) The co-localization of these markers typically demonstrated that α-SMA occupied a position on the exterior of the tube relative to vWF. This indicated that the cell populations expressing endothelial and pericyte markers are separate with the pericyte markers occupying a pericellular position within the growing network.

TEM analysis shown in Figure 7 demonstrated that multiple cells were involved in the formation of extended tubes (Fig. 7A, B) separated by a lumen. A clear lumen within a cellular cross section is evident in Figure 7C and D. The absence of gel material within this lumen suggests that the cells are not simply migrating through the gel simultaneously, but have organized themselves by first establishing the network followed by the formation of a lumen.

### *ASC migration from CSM*

As shown in Figures 8 and 9, cells that had been seeded onto CSM were able to migrate though either PEGylated fibrin (Fig. 8A–C) or collagen (Fig. 8D–F). Migration was seen in both gels as early as day 2 after seeding. Migration and/or proliferation continued throughout the times moni-

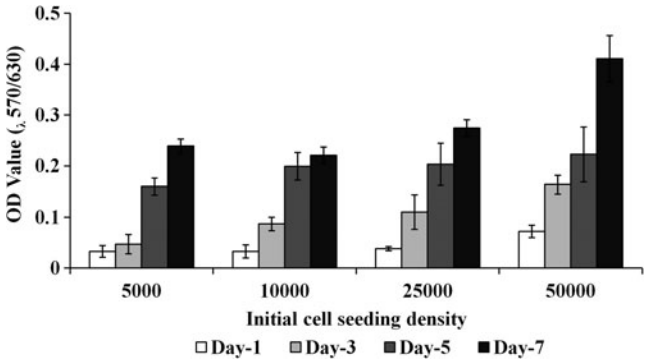


**FIG. 4.** Proliferation of ASC in PEGylated fibrin gels analyzed by MTT (3-(4,5-dimethylthiozole-2-yl)-2,5-diphenyltetrazolium bromide) assay. Viability in comparison to the initial cell seeding density and time (mean optical density [OD] value ± standard deviation, $n = 3$). Cell proliferation and viability increased with increasing cell seeding density.

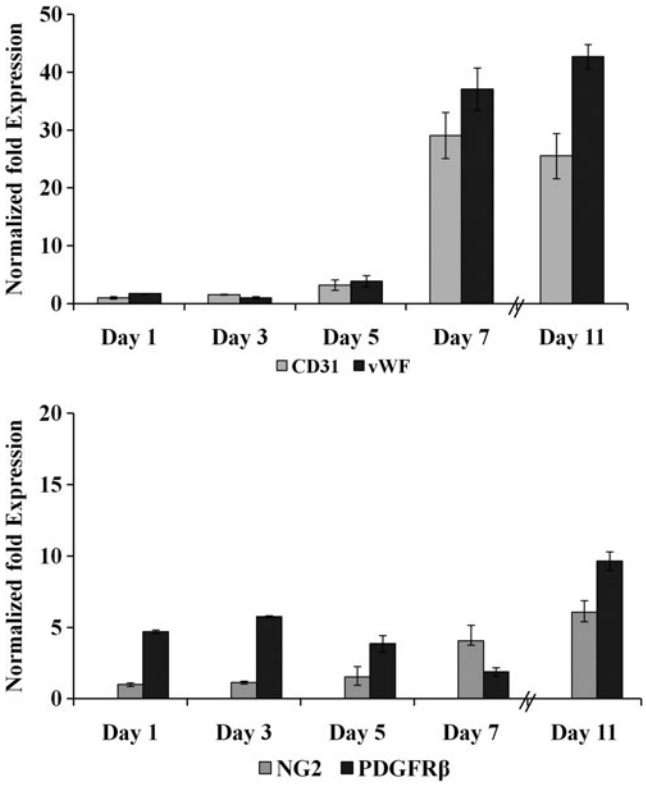


**FIG. 5.** Endothelial and pericyte-specific markers expressed by the differentiated ASC in PEGylated fibrin gels. Expression levels of endothelial cell-specific markers (CD31, von Willebrand factor [vWF]) and pericyte-specific markers (NG2 and platelet-derived growth factor receptor beta [PDGFRβ]) were analyzed using real-time polymerase chain reaction. There was significant increase in endothelial cell-specific markers, CD31 (25-fold) and vWF (42-fold), in comparison to pericyte markers, NG2 (6-fold) and PDGFRβ (9-fold), by day 11.

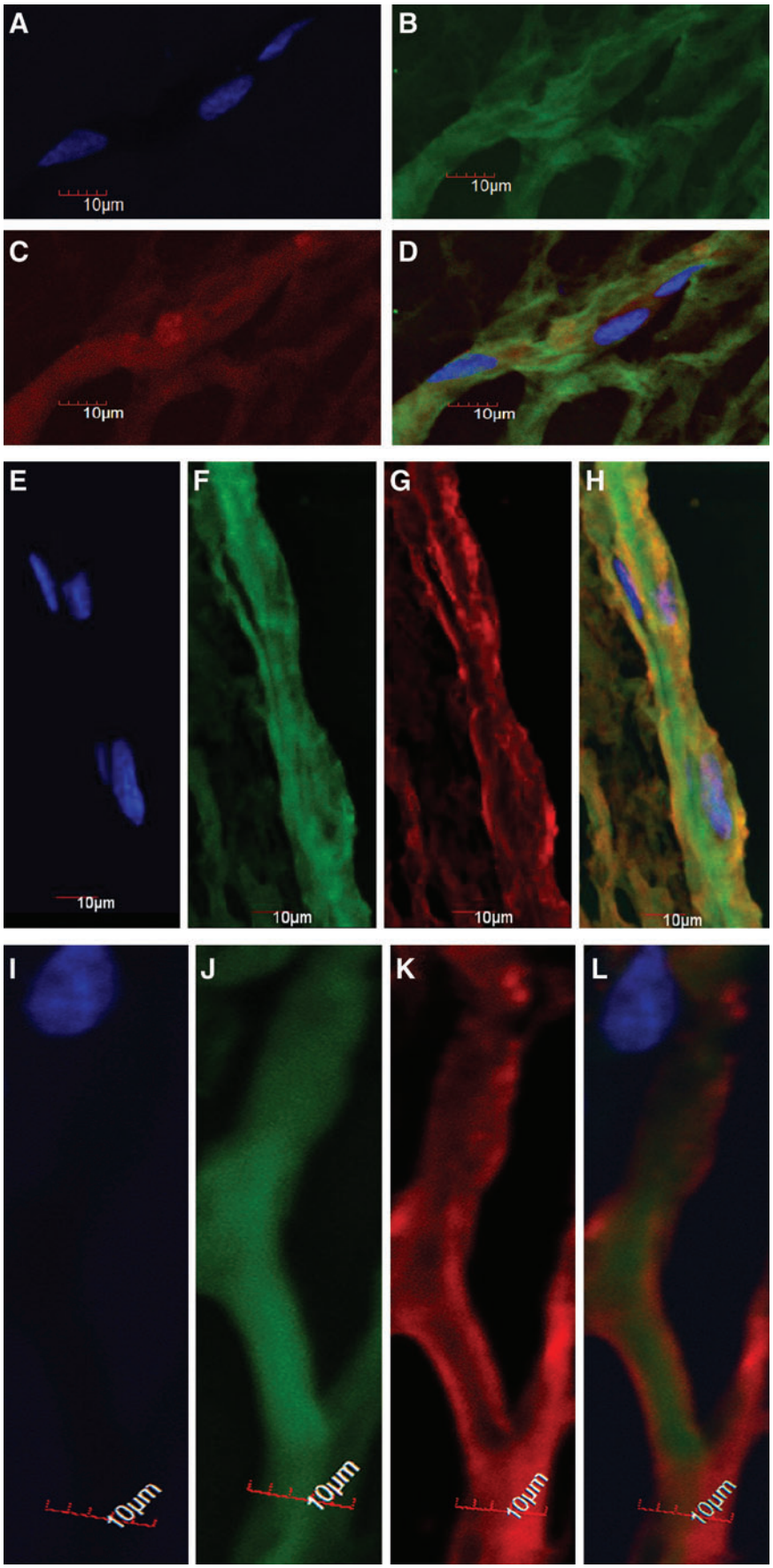


**FIG. 6.** Confocal Z-stacked images of tube-like structures formed by ASC in PEGylated fibrin gel. ASC when seeded in PEGylated fibrin exhibit an endothelial phenotype expressing both vWF **(B)** and CD31 **(C). (D)** The merged image of **(B** and **C)** stained with Hoeschst **(A)** for nuclei. The formed tubes were positive for both pericyte-specific markers NG2 **(G)** and alpha smooth muscle actin (α-SMA) **(K)** and the endothelial cell-specific marker vWF **(F** and **J). (H** and **L)** vWF and Hoeschst **(E** and **I)** merged with NG2 and α-SMA, respectively. Color images available online at www.liebertonline.com/tea.

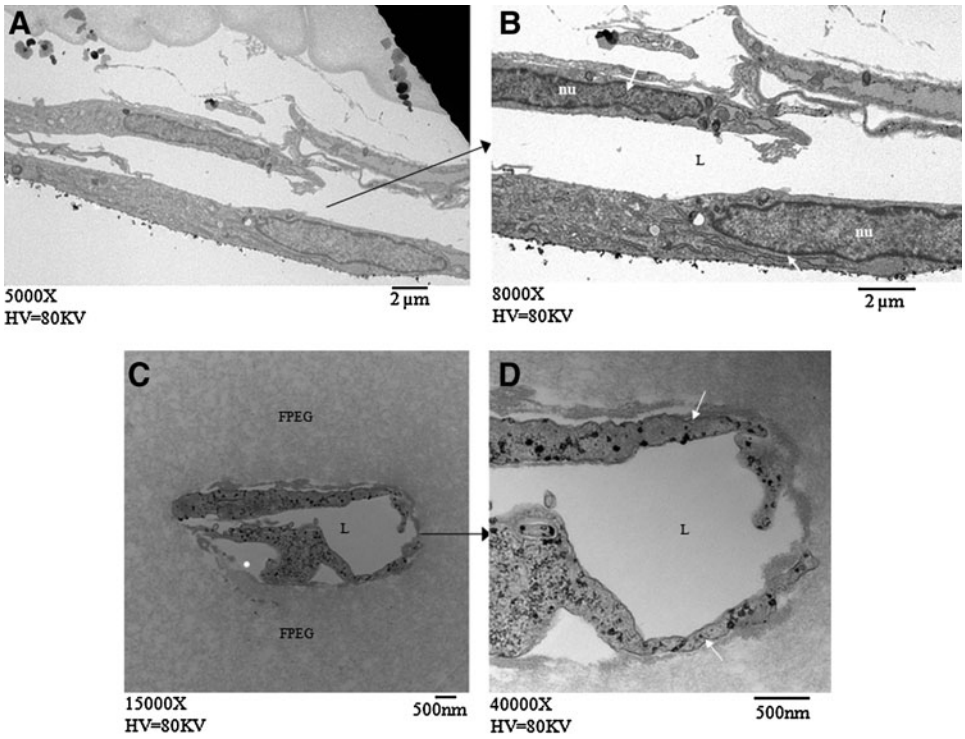


**FIG. 7.** TEM images of ASC forming tube-like structures in PEGylated fibrin following outgrowth from chitosan microspheres (CSM). **(A** and **B)** Two separate cells designated by white arrows that are organized around a lumen (L). The nucleus is designated as nu. **(C** and **D)** A cross section of two separate cells around a lumen that is free of the PEGylated fibrin gel (FPEG). White arrow designates cells involved in lumen formation.

tored (day 8 for PEGylated fibrin and day 12 for collagen). ASC migrating into the PEGylated fibrin demonstrated the characteristic tubular morphology as seen in the gel matrix alone, whereas ASC migrating through the collagen matrix had a spindle-shaped morphology.

When ASC were prelabeled with Qdot 565 nanocrystals and observed after 6 days in culture, the labeled cells could be clearly seen as distinct from the CSM. The fluorescent images as well as the brightfield overlay for migration into both PEGylated fibrin (Fig. 9A–C) and collagen (Fig. 9D–F)

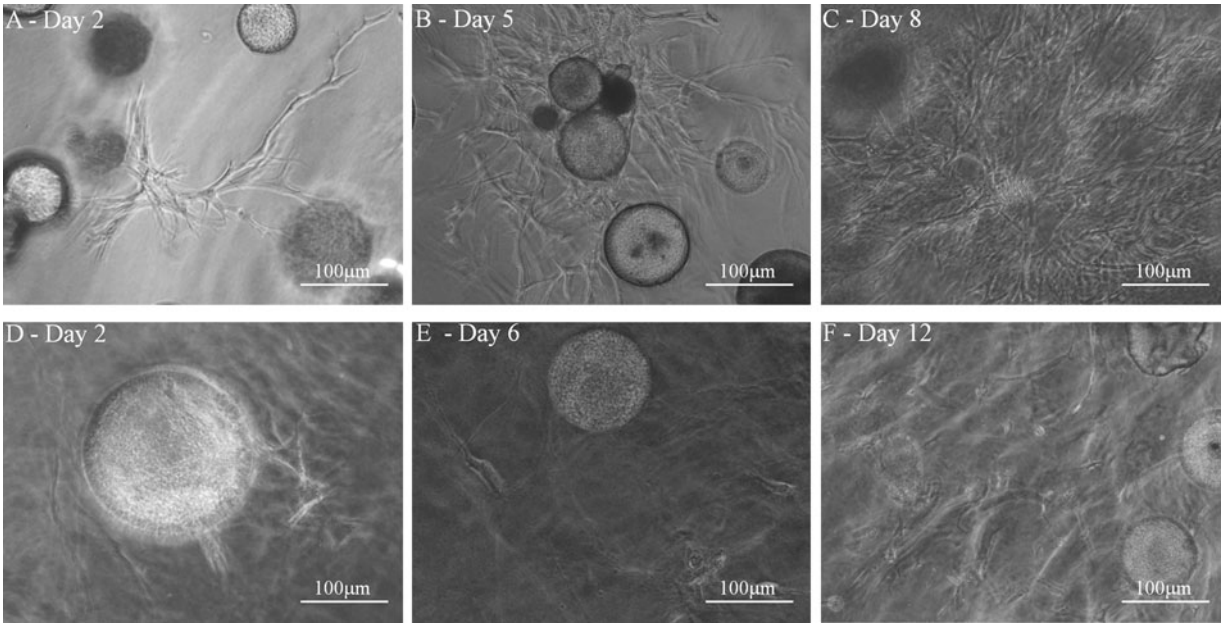


**FIG. 8.** ASC released from CSM *in vitro* in PEGylated fibrin and collagen gels. Phase-contrast images of ASC migrated from CSM into PEGylated fibrin **(A–C)** and collagen **(D–F)**. ASC that have migrated from CSM attached to the PEGylated fibrin shows classical sprouting **(A,** day 2**)** followed by differentiating into tube-like structures **(B,** day 5**)**. Over the time course of differentiation, they migrate into the gel forming a dense multicellular network **(C,** day 8**)**. ASC released from the CSM into collagen were more spindle in appearance **(D,** day 2**)** which developed filopodias **(E,** day 6**)**. Over time they formed more elongated morphological structures stretching along fibril assemblies resembling cells that are associated with stromal tissues.

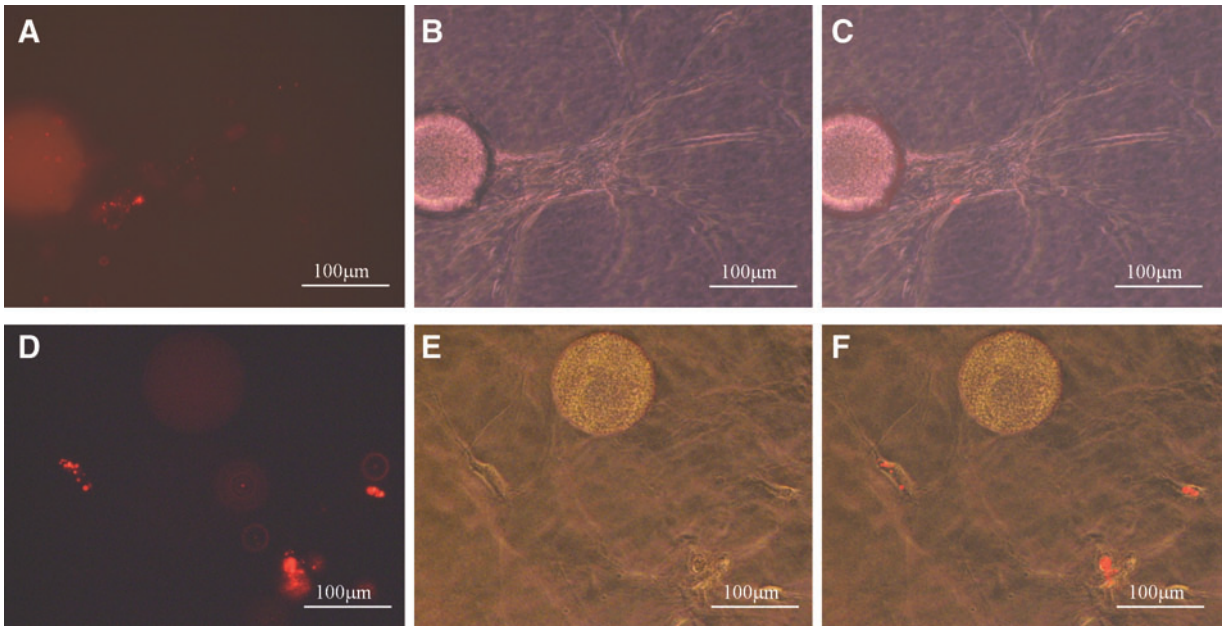


**FIG. 9.** Quantum dot (Qdot) 565-labeled ASC tracked after migration from CSM after day 6 into PEGylated fibrin and collagen gels. Epifluorescent images of Qdot 565–labeled ASC tracked after migration from the CSM into PEGylated fibrin **(A–C)** and collagen **(D–F)** after 6 days. ASC released from CSM into both PEGylated fibrin and collagen could be tracked **(A** and **D)** over 6 days. Cells forming tubes-like structures **(B)** in PEGylated fibrin and striated morphologies **(E)** were colocalized with Qdot 565 **(C** and **F)**. Color images available online at www.liebertonline.com/tea.

are shown. This result provides evidence that the ASC are able to migrate from the embedded microspheres and into either collagen or PEGylated fibrin.

### *Matrix-based morphology of ASC*

Figure 10 consists of a series of light microscopy images over an 11 day time course as ASC grow out of CSM into either collagen or PEGylated fibrin. The cells that had been cultured on the surface of microspheres were sandwiched between the two different gel layers. This type of experimental setup allowed for the independent investigation of the effects that the matrix environment had on cell migration and differentiation. Cells were clearly able to leave the microsphere surface and migrate into either the collagen gel or the PEGylated fibrin. Cells in both gel layers were evident from day 3 until the end of the culture period. The morphology of the migrated ASC were dramatically different in the two gel layers. In the collagen gels, the cells exhibited a spindle-shaped morphology similar to what was seen in the collagen gel layer by itself. In the PEGylated fibrin gels, the cells demonstrated multicellular tubular networks analogous to those in the PEGylated fibrin layer alone. In a number of the figures, it can be clearly seen that the same microsphere population is shown either from the underside (PEGylated fibrin, Fig. 10B, D, and F) or the top side (collagen, Fig. 10A, C, and E). This indicates the proximity of the two cell phenotypes as well as the fact that cells on the same bead can exhibit two distinct phenotypes. The cells in the PEGylated fibrin were able to form extended networks that spanned the dimensions of the acquired image. This result provides evidence for the purely matrix-driven differentiation of ASC in either collagen or PEGylated fibrin.

## Discussion

The goal of this work was to utilize matrix-driven differentiation of ASC for the purpose of simultaneous differentiation toward multiple cell types found in skin, including vascular cells. Toward that end, the proliferation of ASC within PEGylated fibrin gels was demonstrated and quantified. Our prior work detailed the culture and cell phenotype of bone-marrow-derived mesenchymal cells from pig, human, and mouse.[36,46–48] The growth of ASC within PEGylated fibrin is comparable. Work with porcine MSC demonstrated an ~3.5-fold increase in MTT absorbance from days 1 to 3 at a seeding density of 50,000 cells/mL. At the same seeding density, ASC demonstrated approximately a twofold increase in MTT absorbance over the same time period, indicating that cells are able to proliferate within the PEGylated fibrin matrix.

The differentiation of bone marrow MSC has been characterized with respect to gene expression and phenotype.[46] Data demonstrated that an endothelial cell phenotype was expressed by MSC following 3D matrix culture. Additionally, it has previously been reported by our group that the optimum PEG half-life for hydrolysis is ~20 min to enhance vascular differentiation.[46] Various PEG reactive groups were screened and SG-PEG-SG was chosen to produce vascular differentiation due to a similar hydrolysis half-life compared to BTC-PEG-BTC which was used in prior work.[36,47,48] Not only did ASC express endothelial cell phenotype, but also a subset of the ASC expressed pericyte markers. In particular, there was a dramatic upregulation of both CD31 and vWF. This result again parallels what was shown for MSC, with upregulation of CD31 for up to 2 weeks in PEGylated fibrin gels with optimum PEG

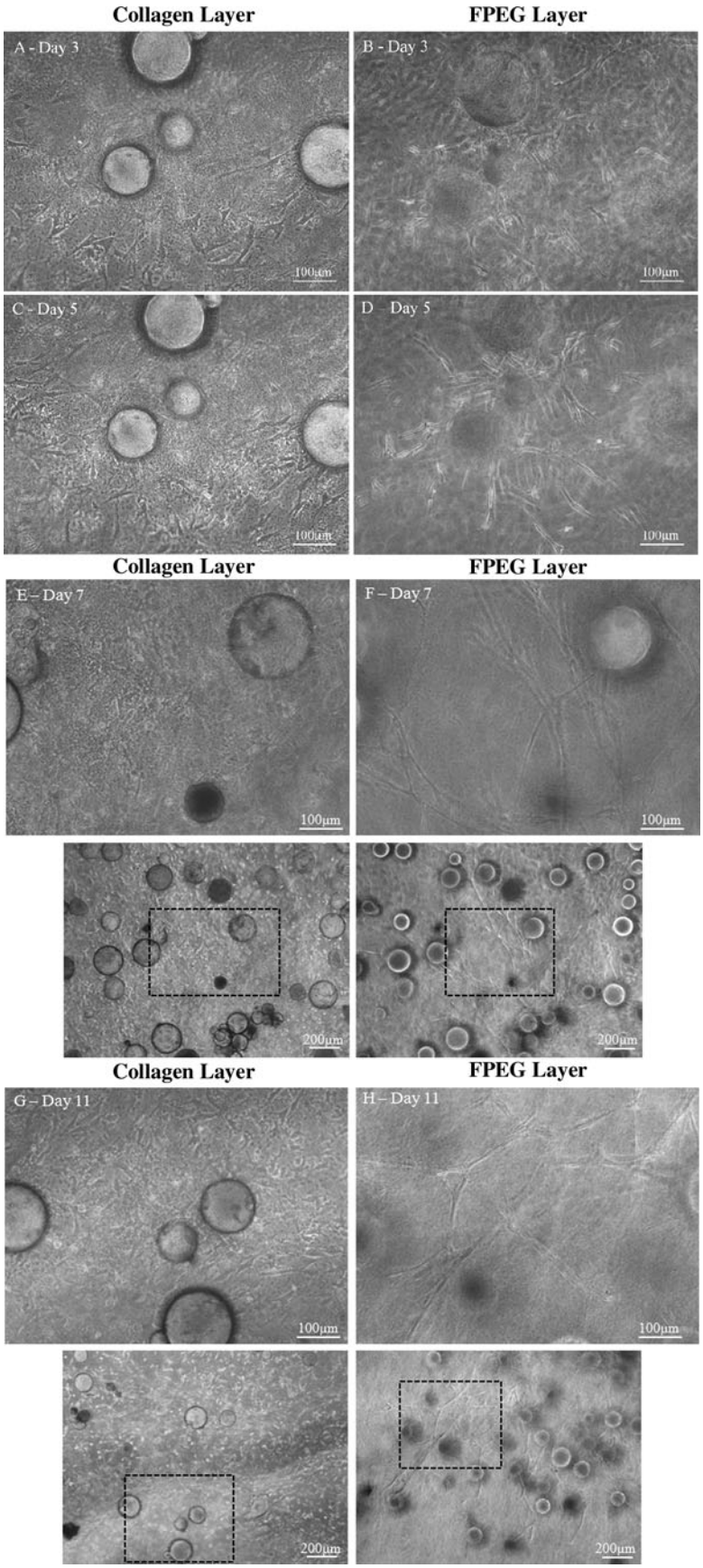


**FIG. 10.** Bidirectional differentiation of ASC in the PEGylated fibrin–(ASC-CSM)–collagen gel constructs. ASC loaded in CSM exhibited matrix-driven phenotypic changes into a fibroblast-like morphology in the collagen layer **(A, C, E,** and **G)** and a tube-like morphology in the PEGylated fibrin layer **(B, D, F,** and **H)** simultaneously. ASC started to migrate into both the gels on day 3 **(A** and **B)** and proliferated as a fibroblast-like phenotype in collagen **(C)** and tube-like sprouts **(D)** in PEGylated fibrin on day 5. By day 7 the collagen layer showed an increase in fibroblast-like cells **(E)**, which eventually populated the gels by day 11 **(G)**. In the PEGylated fibrin layer the sprouts started to form long networks by day 7 **(F)**, which formed complex networks by day 11 **(H)**. Panels below **(E–H)** demonstrate lower magnification view.

hydrolysis rates. This is in contrast to the classical tube formation in Matrigel, where endothelial or other tube-forming cells are allowed to form tubes under defined conditions. This assay has been used to demonstrate endothelial cell phenotype, but tubes typically regress before the 2 week time point.[49]

With respect to pericyte gene and protein expression, NG2 mRNA was upregulated over the time course studied with corresponding evidence for the cell surface marker. PDGFRβ gene expression, however, was more complex. While the growth factor receptor is a known marker for pericytes in developing blood vessels, it is also found expressed on undifferentiated MSC.[50] PDGF-BB is secreted by angiogenic endothelial cells (i.e., endothelial cells actively proliferating and undergoing morphogenesis to form patent tubes). This chemokine serves as a mitogen for pericytes. Although PDGF-BB is expressed by several cell types, the PDGFRβ is expressed on pericytes. Supporting the importance of interactions between PDGF-BB and PDGFRβ are studies from *Pdgfb* knockout mice. These mice lack pericytes on select vessels and demonstrate microvascular aneurysms and ultimately result in embryonic lethality.[51] In addition, deletion of the retention motif of PDGF-BB results in defective investment of pericytes in the microvessel wall and severely impairs renal and retinal function in adult mice.[51] What has been shown in the current work is a decrease of the receptor expression as the multipotent ASC differentiates up to day 7. The increase of receptor expression at day 11 is likely due to the enhanced pericyte gene expression with corroborating evidence from NG2 gene expression enhancement.

It was postulated in the present study that in light of the recent understanding of the perivascular location of MSC from multiple tissues,[52] it may be critical to characterize pericyte differentiation in addition to endothelial cell differentiation. Results from the present study demonstrate that not only is gene expression for pericyte markers upregulated, although not to the extent that endothelial cell markers are, but also the proteins are expressed in a distinct morphology. Both NG2 and α-SMA are seen in a perivascular position relative to the endothelial marker, vWF. This result gives evidence that not only is there a subpopulation of ASC that express pericyte phenotype, but there is also physical organization of the two subpopulations relative to the tubular networks in a manner that would be expected for a growing vascular network.

The purpose of the CSM in this study is twofold. The first is primarily technical in that it was desirable in this study to localize the cells to the interface between the collagen and PEGylated fibrin gels. This allowed for the microscopic localization of the interface as the microspheres do not migrate between the gel layers. It was then possible to evaluate whether the ASC had a preference for migrating within either the collagen or PEGylated fibrin gels. Further, this technique allowed for a greater degree of certainty in evaluating cell phenotype within either the collagen or PEGylated fibrin layers. Future studies will allow for tube length to be quantified from the microsphere as a point of origin. The second use of the CSM was to provide a convenient method for cell delivery either in combination with different hydrogel matrices, such as collagen and PEGylated fibrin in the current work, or in a layered assembly designed to approximate the layered structure of skin. The cell-loaded CSM allow for the precise and uniform localization of delivered ASC.

Our prior work has demonstrated that ASC loaded onto CSM could migrate into a collagen gel and, in particular, that their differentiation potential toward adipocytes and osteoblasts was maintained after migration from the microspheres.[45] Further, this carrier has been optimized with respect to composition and cell loading characteristics, and the optimized configuration has been employed here. Results from the current work demonstrate that ASC migration is possible from the CSM into either collagen or PEGylated fibrin gels. ASC are able to proliferate within both of these gel matrices; however, differentiation is greatly enhanced in the PEGylated fibrin gels. Cell morphology is dramatically different in the two different gel types even within the same construct. This provides further evidence for matrix-driven differentiation that is independent of soluble factors or cytokines.

This work demonstrates that matrix characteristics can be used to control ASC specification toward a vascular phenotype. Further, multiple gel matrices can be used in combination with a cell carrier delivery system. Cells are able to migrate from the microsphere carriers and proliferate within either collagen or PEGylated fibrin gels. Under the same culture conditions, cell genotype and phenotype was solely dictated by the matrix microenvironment. This work provides direct evidence for the importance of the extracellular matrix in directing stem cell phenotype as well as provides a template for the creation of layered composites as wound healing dressings or artificial skin.

## Acknowledgments

The authors would like to thank Ms. Janet Roe for isolation of adipose tissue and technical support. S. Natesan is supported by a Postdoctoral Fellowship Grant from the Pittsburgh Tissue Engineering Initiative. Confocal images were generated in the core optical imaging facility, which is supported by the University of Texas Health Science Center, San Antonio, TX, NIH-NCI P30 CA54174 (San Antonio Cancer Institute), NIH-NIA P30 AG013319 (Nathan Shock Center, San Antonio, TX), and NIH-NIA P01AG19316. Funding for this work was provided by the Telemedicine and Advanced Technology Research Center (TATRC) at the U.S. Army Medical Research and Materiel Command (USAMRMC) through award W81XWH-09-2-0103 and the Deployment Related Medical Research Program (DRMRP) through award W81XWH-09-1-0607. The authors thank Dr. Robert Reddick, Medical Director, and Lauren Chesnut, Technical Director of the Electron Microscopy Facility at The University of Texas Health Science Center, Department of Pathology, for use of facility and assistance in the analysis of electron micrographs (EM).

## Disclosure Statement

The opinions or assertions contained herein are the private views of R.J.C., D.G.B., and T.J.W. and are not to be construed as official or as reflecting the views of the Department of the Army or the Department of Defense.

## References

1. Ehrenreich, M., and Ruszczak, Z. Tissue-engineered temporary wound coverings. Important options for the clinician. Acta Dermatovenerol Alp Panonica Adriat **15,** 5, 2006.
2. Mansbridge, J. Skin tissue engineering. J Biomater Sci Polym Ed **19,** 955, 2008.

3. Ehrenreich, M., and Ruszczak, Z. Update on tissue-engineered biological dressings. Tissue Eng **12,** 2407, 2006.
4. Zhang, C.P., and Fu, X.B. Therapeutic potential of stem cells in skin repair and regeneration. Chin J Traumatol **11,** 209, 2008.
5. Ogawa, R. The importance of adipose-derived stem cells and vascularized tissue regeneration in the field of tissue transplantation. Curr Stem Cell Res Ther **1,** 13, 2006.
6. Sandor, G.K., and Suuronen, R. Combining adipose-derived stem cells, resorbable scaffolds and growth factors: an overview of tissue engineering. J Can Dent Assoc **74,** 167, 2008.
7. Brzoska, M., *et al.* Epithelial differentiation of human adipose tissue-derived adult stem cells. Biochem Biophys Res Commun **330,** 142, 2005.
8. Planat-Benard, V., *et al.* Plasticity of human adipose lineage cells toward endothelial cells: physiological and therapeutic perspectives. Circulation **109,** 656, 2004.
9. Romanov, Y.A., *et al.* Mesenchymal stem cells from human bone marrow and adipose tissue: isolation, characterization, and differentiation potentialities. Bull Exp Biol Med **140,** 138, 2005.
10. Sgodda, M., *et al.* Hepatocyte differentiation of mesenchymal stem cells from rat peritoneal adipose tissue *in vitro* and *in vivo*. Exp Cell Res **313,** 2875, 2007.
11. Zuk, P.A., *et al.* Multilineage cells from human adipose tissue: implications for cell-based therapies. Tissue Eng **7,** 211, 2001.
12. Aust, L., *et al.* Yield of human adipose-derived adult stem cells from liposuction aspirates. Cytotherapy **6,** 7, 2004.
13. Kim, W.S., *et al.* Wound healing effect of adipose-derived stem cells: a critical role of secretory factors on human dermal fibroblasts. J Dermatol Sci **48,** 15, 2007.
14. Mosesson, M.W. Fibrinogen and fibrin structure and functions. J Thromb Haemost **3,** 1894, 2005.
15. Jockenhoevel, S., *et al.* Fibrin gel—advantages of a new scaffold in cardiovascular tissue engineering. Eur J Cardiothorac Surg **19,** 424, 2001.
16. Cho, S.W., *et al.* Enhancement of adipose tissue formation by implantation of adipogenic-differentiated preadipocytes. Biochem Biophys Res Commun **345,** 588, 2006.
17. Birla, R.K., *et al.* Myocardial engineering *in vivo*: formation and characterization of contractile, vascularized three-dimensional cardiac tissue. Tissue Eng **11,** 803, 2005.
18. Long, J.L., and Tranquillo, R.T. Elastic fiber production in cardiovascular tissue-equivalents. Matrix Biol **22,** 339, 2003.
19. Mol, A., *et al.* Fibrin as a cell carrier in cardiovascular tissue engineering applications. Biomaterials **26,** 3113, 2005.
20. Ye, Q., *et al.* Fibrin gel as a three dimensional matrix in cardiovascular tissue engineering. Eur J Cardiothorac Surg **17,** 587, 2000.
21. Alaminos, M., *et al.* Construction of a complete rabbit cornea substitute using a fibrin-agarose scaffold. Invest Ophthalmol Vis Sci **47,** 3311, 2006.
22. Han, B., *et al.* A fibrin-based bioengineered ocular surface with human corneal epithelial stem cells. Cornea **21,** 505, 2002.
23. Suuronen, E.J., *et al.* Promotion of angiogenesis in tissue engineering: developing multicellular matrices with multiple capacities. Int J Artif Organs **29,** 1148, 2006.
24. Hecker, L., *et al.* Development of a three-dimensional physiological model of the internal anal sphincter bioengineered *in vitro* from isolated smooth muscle cells. Am J Physiol Gastrointest Liver Physiol **289,** G188, 2005.
25. Huang, Y.C., *et al.* Rapid formation of functional muscle *in vitro* using fibrin gels. J Appl Physiol **98,** 706, 2005.
26. Nieponice, A., *et al.* Mechanical stimulation induces morphological and phenotypic changes in bone marrow-derived progenitor cells within a three-dimensional fibrin matrix. J Biomed Mater Res A **81,** 523, 2007.
27. Rowe, S.L., Lee, S., and Stegemann, J.P. Influence of thrombin concentration on the mechanical and morphological properties of cell-seeded fibrin hydrogels. Acta Biomater **3,** 59, 2007.
28. Balestrini, J.L., and Billiar, K.L. Equibiaxial cyclic stretch stimulates fibroblasts to rapidly remodel fibrin. J Biomech **39,** 2983, 2006.
29. Hojo, M., *et al.* Induction of vascular endothelial growth factor by fibrin as a dermal substrate for cultured skin substitute. Plast Reconstr Surg **111,** 1638, 2003.
30. Martineau, L., and Doillon, C.J. Angiogenic response of endothelial cells seeded dispersed versus on beads in fibrin gels. Angiogenesis **10,** 269, 2007.
31. Nehls, V., Schuchardt, E., and Drenckhahn, D. The effect of fibroblasts, vascular smooth muscle cells, and pericytes on sprout formation of endothelial cells in a fibrin gel angiogenesis system. Microvasc Res **48,** 349, 1994.
32. Potter, M.J., *et al.* An investigation to optimize angiogenesis within potential dermal replacements. Plast Reconstr Surg **117,** 1876, 2006.
33. Liu, H., Collins, S.F., and Suggs, L.J. Three-dimensional culture for expansion and differentiation of mouse embryonic stem cells. Biomaterials **27,** 6004, 2006.
34. Liu, J., *et al.* Autologous stem cell transplantation for myocardial repair. Am J Physiol Heart Circ Physiol **287,** H501, 2004.
35. Pittenger, M.F., *et al.* Multilineage potential of adult human mesenchymal stem cells. Science **284,** 143, 1999.
36. Zhang, G., *et al.* A PEGylated fibrin patch for mesenchymal stem cell delivery. Tissue Eng **12,** 9, 2006.
37. Ennett, A.B., and Mooney, D.J. Tissue engineering strategies for *in vivo* neovascularisation. Expert Opin Biol Ther **2,** 805, 2002.
38. Mandinov, L., *et al.* Copper chelation represses the vascular response to injury. Proc Natl Acad Sci U S A **100,** 6700, 2003.
39. Post, M.J., and Simons, M. The rational phase of therapeutic angiogenesis. Minerva Cardioangiol **51,** 421, 2003.
40. Zuk, P.A., *et al.* Human adipose tissue is a source of multipotent stem cells. Mol Biol Cell **13,** 4279, 2002.
41. Mosmann, T. Rapid colorimetric assay for cellular growth and survival: application to proliferation and cytotoxicity assays. J Immunol Methods **65,** 55, 1983.
42. Barthel, L.K., and Raymond, P.A. Improved method for obtaining 3-microns cryosections for immunocytochemistry. J Histochem Cytochem **38,** 1383, 1990.
43. Chomczynski, P., and Sacchi, N. Single-step method of RNA isolation by acid guanidinium thiocyanate-phenol-chloroform extraction. Anal Biochem **162,** 156, 1987.
44. Livak, K.J., and Schmittgen, T.D. Analysis of relative gene expression data using real-time quantitative PCR and the 2(-Delta Delta C(T)) Method. Methods **25,** 402, 2001.
45. Natesan, S., *et al.* Adipose-derived stem cell delivery into collagen gels using chitosan microspheres. Tissue Eng Part A **16,** 1369, 2010.
46. Zhang, G., *et al.* Vascular differentiation of bone marrow stem cells is directed by a tunable three-dimensional matrix. Acta Biomater **6,** 3395, 2010.
47. Zhang, G., *et al.* Enhancing efficacy of stem cell transplantation to the heart with a PEGylated fibrin biomatrix. Tissue Eng Part A **14,** 1025, 2008.
48. Zhang, G., *et al.* Controlled release of stromal cell-derived factor-1 alpha *in situ* increases c-kit+ cell homing to the infarcted heart. Tissue Eng **13,** 2063, 2007.

49. Kubota, Y., *et al.* Role of laminin and basement membrane in the morphological differentiation of human endothelial cells into capillary-like structures. J Cell Biol **107,** 1589, 1988.
50. Amos, P.J., *et al.* IFATS collection: the role of human adipose-derived stromal cells in inflammatory microvascular remodeling and evidence of a perivascular phenotype. Stem Cells **26,** 2682, 2008.
51. Lindblom, P., *et al.* Endothelial PDGF-B retention is required for proper investment of pericytes in the microvessel wall. Genes Dev **17,** 1835, 2003.
52. Caplan, A.I. All MSCs are pericytes? Cell Stem Cell **3,** 229, 2008.

Address correspondence to:
*Laura J. Suggs, Ph.D.*
*Department of Biomedical Engineering*
*The University of Texas at Austin*
*1 University Station, C0800*
*Austin, TX 78712-0238*

*E-mail:* laura.suggs@mail.utexas.edu

*Received: May 17, 2010*
*Accepted: November 11, 2010*
*Online Publication Date: December 28, 2010*